A transposable element into the human long noncoding RNA CARMEN is a switch for cardiac precursor cell specification

Isabelle Plaisance, Panagiotis Chouvardas, Yuliangzi Sun, Mohamed Nemir, Parisa Aghagolzadeh, Farhang Aminfar, Sophie Shen, Woo Jun Shim, Francesca Rochais, Rory Johnson, et al.

A transposable element into the human long noncoding RNA *CARMEN* is a switch for cardiac precursor cell specification

Isabelle Plaisance[a], Panagiotis Chouvardas[b], Yuliangzi Sun[c], Mohamed Nemir[a], Parisa Aghagolzadeh[a], Farhang Aminfar[a], Sophie Shen[c], Woo Jun Shim[c], Francesca Rochais[d], Rory Johnson[b,e], Nathan Palpant[c], Thierry Pedrazzini[a, f]

[a]Experimental Cardiology Unit, Division of Cardiology, University of Lausanne Medical School, Lausanne, Switzerland; [b]Department of Medical Oncology, Inselspital, University of Bern, Bern, Switzerland; [c]Institute for Molecular Bioscience, University of Queensland, Brisbane, Australia; [d]Aix Marseille University, INSERM, MMG, U1251, Marseille, France; [e]School of Biology and Environmental Science, University College Dublin, Dublin, Ireland;

[f] Correspondence to:
Thierry Pedrazzini, Experimental Cardiology Unit, Division of Cardiology, Department of Cardiovascular Medicine, University of Lausanne Medical School, Lausanne, Switzerland
Email: thierry.pedrazzini@chuv.ch
Phone: +41 21 314 0765

Short title: A molecular switch encoded in a long noncoding RNA

Original article: 8672 words

ABSTRACT

Aims: The major cardiac cell types composing the adult heart arise from common multipotent precursor cells. Cardiac lineage decisions are guided by extrinsic and cell-autonomous factors, including recently discovered long noncoding RNAs (lncRNAs). The human lncRNA *CARMEN* , which is known to dictate specification towards the cardiomyocyte (CM) and the smooth muscle cell (SMC) fates, generates a diversity of alternatively spliced isoforms.

Methods and Results: The *CARMEN* locus can be manipulated to direct human primary cardiac precursor cells (CPCs) into specific cardiovascular fates. Investigating *CARMEN* isoform usage in differentiating CPCs represents therefore a unique opportunity to uncover isoform-specific function in lncRNAs. Here, we identify one CARMEN isoform, *CARMEN-201,* to be crucial for SMC commitment. *CARMEN-201* activity is encoded within an alternatively-spliced exon containing a MIRc short interspersed nuclear element. This element binds the transcriptional repressor REST (RE1 Silencing Transcription Factor), targets it to cardiogenic loci, including *ISL1*, *IRX1*, *IRX5*, and *SFRP1*, and thereby blocks the CM gene program. In turn, genes regulating SMC differentiation are induced.

Conclusions: These data show how a critical physiological switch is wired by alternative splicing and functional transposable elements in a long noncoding RNA. They further demonstrated the crucial importance of the lncRNA isoform *CARMEN-201* in SMC specification during heart development.

TRANSLATIONAL PERSPECTIVE

LncRNAs regulate cell commitment and differentiation during development. Taking advantage of cardiac precursor cells isolated from the human fetal and adult heart, we identify a novel mechanism mediated by a specific isoform of the lncRNA *CARMEN*, which controls specification into the smooth muscle cell vs. the cardiomyocyte fate. These results have direct implication in cell therapy for heart disease. Moreover, *CARMEN* is associated with pathological states and represents an interesting biomarker for assessing the extent of damage in the cardiovascular system. Our data propose therefore a mean to control cardiac cell identity and behavior during heart development and disease.

KEY WORDS

Cardiac precursor cells; smooth muscle cells; long noncoding RNAs; Splicing; Transposable elements

INTRODUCTION

The mammalian heart is composed of several cell types that derives from mesodermal progenitor cells of the first and second heart field [1]. The distinct lineages arise from multipotent cardiovascular precursors [2-4]. In this framework, very few studies have evaluated transcriptional regulation in primary human cardiac precursor cells (CPCs). We have previously derived clonal populations of CPCs from the fetal and the adult human heart [5, 6]. Their comparison allows for the dissection of the molecular mechanisms controlling cardiac specification and differentiation. Understanding the processes regulating cardiac cell programming and reprogramming provides also novel insights for the treatment of cardiovascular disease.

Next generation sequencing coupled to assessment of the epigenetic landscape has shown that mammalian genomes produce thousands of noncoding transcripts. Of these, long noncoding (lnc)RNAs represent the most heterogeneous and diverse class of RNA molecules. LncRNAs can be multiexonic, spliced, capped and polyadenylated [7]. Current estimates predict the existence of approximately 200,000 lncRNAs in human, of which very few have been fully characterized. LncRNAs are implicated in a variety of functions that define cell identity and behavior. They exert *Cis*- and *Trans*-regulatory functions, controlling chromatin remodeling and transcription. *Cis*-acting lncRNAs operate at a close vicinity to their site of transcription [8]. On the other hand, *Trans*-acting lncRNAs leave their site of transcription and exert functions at remote locations in the genome [9]. In this case, lncRNAs partner with proteins such as chromatin remodelers to modify the local chromatin environment at target locations. In the cardiovascular system, several lncRNAs have been identified as key players of cell differentiation and homoeostasis. *Braveheart*, *Fendrr* and *Meteor* have been involved in mesoderm and cardiac differentiation [10-12]. *Myheart* controls CM hypertrophy, and *Wisper* is a regulator of cardiac fibroblasts, critical for the development of fibrosis [13, 14]. Then, *SMILR* and *SENCR* have been associated with SMC proliferation and differentiation [15, 16].

The way in which functions are encoded in lncRNAs' sequences remains enigmatic. It is thought that lncRNAs comprise modular assemblages of functional elements, composed of structural motifs that interact with proteins or other nucleic acids [17]. Recent studies have implicated repetitive transposable elements as a source of functional lncRNA domains [18, 19]. In this context, lncRNA loci can produce a

variety of transcripts through alternative splicing [7, 20]. It has been speculated that these alternative isoforms, by containing different combinations of exon sequences, thereby exert diverse functions. Some years ago, we identified *CARMEN*, a conserved lncRNA essential for cardiogenesis [21]. *CARMEN* has been previously referred to as *MIR143HG* because the locus hosts *MIR-143* and *MIR-145*, two microRNAs (miRNAs) important for SMC differentiation [22]. Nevertheless, the miRNA precursor represents only one *CARMEN* isoform among several others. All other isoforms are lncRNA splice variants, with no apparent coding potential, for which functions remain to be fully defined. We showed previously that three isoforms were involved in cardiac specification in human fetal CPCs [21]. Moreover, we reported that one isoform, referred earlier as to *CARMEN-7* (formally *CARMEN-201* or ENST00000505254), was differentially expressed in CPCs committing to the CM vs. the SMC lineage [6]. Interestingly, the *CARMEN* locus can be manipulated to direct CPCs into specific cardiovascular fates. Investigating *CARMEN* isoform usage in differentiating CPCs represents therefore a unique opportunity to uncover isoform-specific function in lncRNAs. Here, we demonstrate that *CARMEN-201* controls specification into the SMC lineage in human CPCs, and that this function is encoded within an alternatively-spliced exon containing a MIRc short interspersed nuclear element.

METHODS

Methods are described in details in the Supplementary Information available online.

Human cardiac precursor cells (CPCs)

Fetal heart biopsies were collected at 5 weeks of gestation following abortion, and adult atrial appendages were obtained from patients undergoing cardiac surgery. CPCs were isolated by enzymatic digestion as previously described [5, 6].

Human plasma samples

Plasma samples were collected from patients admitted to the Lausanne University Hospital with a diagnosis of myocardial infarction.

Study approval

The study was approved by the Lausanne University Hospital Ethics Committee and the Swiss Ethics Committee (Human cardiac precursor cells: Protocols 22/03 and 178/09; Human plasma from patients with myocardial infarction: Protocol PB_2018-00231 and 94/15), and was conducted according to the Declaration of Helsinki. Written informed consent was obtained from all patients included in the study.

GapmeR-mediated knockdown

CARMEN-201 silencing was obtained by adding *CARMEN-201*-specific GapmeRs targeting Exon 2 to CPCs at a final concentration of 20 nM.

siRNA-mediated knockdown

siRNA transfection was performed using RNAiMax (ThermoFisher). CPCs were transfected with the indicated siRNA at a final concentration of 10 nM.

RNA extraction, RT-PCR and real time PCR

Total RNA from plasma and from cultured cells was extracted using the miRNeasy Serum/Plasma Advanced kit and the miRNeasy kit (Qiagen).

Absolute quantification of CARMEN isoform expression

pBluescript SK+ plasmids containing *CARMEN-201*, *CARMEN-205* or *CARMEN-217* cDNA were synthesized (GenScript, USA). Data were converted into transcript copy per cell, assuming 100% efficiency in conversion of RNA into cDNA.

Subcellular fractionation

Cells were harvested and lysed. The lysate was centrifuged at 3800g for 2 min. The supernatant represented the cytoplasmic fraction. The pellet was used to produce the nuclear fraction.

CRISPR/Cas9-mediated Exon 2 deletion

A CRISPR/Cas9-D10A Nickase-based strategy was used to delete Exon 2 in the *CARMEN* gene.

CRISPR-On activation

We used the CRISPR/dCas9-based Synergistic Activator Mediator (SAM) gain of function system to activate *CARMEN* isoform expression in fetal CPCs [23].

RNA sequencing

Sequencing libraries were prepared according to Illumina RNA Seq library kit instructions. Libraries were sequenced with the Illumina HiSeq2000 (100bp; PE).

TRIAGE analysis

The Transcriptional Regulatory Inference Analysis from Gene Expression (TRIAGE) analysis, providing a means to identify cell type-specific regulatory genes has been described [24].

Uniform Manifold Approximation and Projection (UMAP) density plots

We used the data provided by Asp et al., 2019 (accession number is European Genome-phenome Archive (EGA): EGAS00001003996). The UMAP were generated using *Nebulosa* package.

Lentiviral vectors

The SIN-cppt-CMV-EGFP-WHV plasmid was a kind gift of Dr. Nicole Deglon (University of Lausanne, Lausanne, Switzerland). EGFP sequences were replaced by either the wild-type CARMEN-201 Exon 2 or a mutated Exon 2 containing scrambled MIRc sequences.

RNA Pulldown and identification of *CARMEN-201* protein partners

The pBluescript SK+ plasmids containing *C-201* Ex2 or *C-201* mutEx2 were used to synthetize biotinylated probes. Precleared lysate was incubated with either no probe, biotinylated *C-201* Ex2 or biotinylated mut*C-201* Ex2. Proteins were loaded on 12% SDS-PAGE.

Tandem mass spectrometry

For identifying *CARMEN-201* protein partners, tryptic peptide mixtures were injected on an Ultimate RSLC 3000 nanoHPLC system (Dionex, Sunnyvale, CA, USA).

Western blotting

Proteins associated to biotinylated C-201 transcript were resolved by SDS-PAGE and electroblotted onto PVDF membranes (GE Healthcare).

RNA Immunoprecipitation (RIP)

The RIP experiment was conducted as described [14].

RIP following by sequencing

RIP was performed using anti-REST IgG. REST-associated transcripts were purified using the RNeasy isolation kit (Qiagen). Sequencing libraries were prepared according to Illumina RNA Seq library kit instructions. Libraries were sequenced with the Illumina HiSeq2000 (100bp; PE).

Chromatin immunoprecipitation followed by real-time quantitative PCR (ChIP-qPCR)

ChIP-qPCR was performed using the Pierce magnetic ChIP Kit (Thermo Scientific) and the ChIPAb+ REST Kit (Millipore) according to the manufacturers' instructions.

Immunohistochemistry

Cells were fixed in 2% paraformaldehyde, permeabilized in 0.3% Triton-X100 and processed for immunostaining using appropriate antibodies. Coverslips were mounted with VECTASHIELD Antifade Mounting medium with DAPI (VECTOR LABORATORIES).

RNA BaseScope in situ hybridization

RNA BaseScope in situ hybridization was used to detect *CARMEN-201* expression in adult CPCs in culture or in sections of human hearts. In situ detection was performed the BaseScope kit (ACD biotech, 323900).

Masson's trichome staining

Paraffin tissue sections were also processed for Masson's trichrome staining and analyzed with a Zeiss Axioscan Z1 (Carl Zeiss).

Statistics

All data were collected from at least 3 independent experiments, performed at least in triplicates. Data throughout the paper are expressed as mean ± SEM. Statistical analysis: ANOVA with post-hoc Tukey.

RESULTS

CARMEN isoforms are differentially expressed in CPCs committing to the CM vs. the SMC fate.

To study the importance of *CARMEN* isoforms in cardiac differentiation, we took advantage of primary CPCs isolated from the human heart. We isolated CPCs from the fetal heart at 5 weeks of gestation, hereafter referred to as fetal CPCs [5]. Adult CPCs were isolated from atrial appendages of cardiac patients [6]. Fetal CPCs have a high propensity to differentiate into CMs whereas adult CPCs preferentially produce SMCs. Indeed, seven days after inducing differentiation, CMs, expressing *ACTN2*, *ACTC1*, *MYH6*, *MYH7* and *TNN1*, were readily detected in fetal CPC cultures. In contrast, adult CPCs differentiated into SMCs expressing *ACTA2*, *CALD1*, *CNN1* and *MYH11* (Fig. 1a and b; Supplemental Fig.

S1a). We next analyzed *CARMEN* expression under these two experimental conditions. Using capture long-read sequencing [25], we detected seven annotated isoforms, i.e. *CARMEN (C)-201*, *-202*, *-205*, *-210*, *-212*, *-215*, and *-217* (GENCODE v33; Fig. 1c). *C-215* is the precursor of *MIR-143* and *MIR145* whereas all other isoforms represent lncRNA transcripts whose expression terminates upstream of the miRNAs. All isoforms were significantly expressed in adult CPCs during SMC differentiation. In contrast, one isoform, *C-201*, was downregulated during differentiation of fetal CPCs into CMs (Supplemental Fig. S1b). Absolute quantification confirmed *C-201* represented the main isoform in adult CPCs but the least abundant in fetal CPCs (Fig. 1d), suggesting its involvement in SMC differentiation. All *CARMEN* isoforms but the miRNA precursor (*C-215*) were more abundant in the nucleus than the cytoplasm, a feature compatible with the postulated function of lncRNAs as regulators of gene expression (Fig. 1e; Supplemental Fig. S1c).

CARMEN-201 controls SMC specification via its second exon

We next evaluated the involvement of *C-201* in SMC differentiation using a knockdown approach. Antisense oligonucleotides (GapmeRs) were designed to target the *C-201* second exon, uniquely present in this isoform (Fig. 1c). *C-201* was downregulated in adult CPCs following GapmeR transfection (Supplemental Fig. S2a). The anti-*C-201* GapmeRs affected no other isoforms, demonstrating the specificity of the approach. *C-201* silencing had no effects on differentiation of fetal CPCs into CMs but completely blocked the capacity of adult CPCs to produce SMCs (Supplemental Fig. S2b and c). To explore the importance of the *C-201* second exon in SMC specification, we produce adult CPCs lacking the exon using CRISPR/Cas9 deletion. Guide (g)RNAs were designed to remove the second exon without affecting any other exons (Supplemental Fig. S3a). *C-201* Exon 2-deleted adult CPC clones were derived. Importantly, the *C-201* isoform was still expressed in adult CPCs lacking *C-201* Exon 2. However, the transcript was reduced by the size of the second exon (Supplemental Fig. S3b). Endogenous *C-201* expression was similarly induced in both wild-type and deleted adult CPC (Δ201Ex2) clones during differentiation as detected by using a primer pair amplifying the 3' end of the transcript (Fig. 1f; primer pair P1). The deletion of the second exon was verified using two primer pairs spanning the exon (i.e. P2; P3). Next, we evaluated the capacity of deleted adult CPCs to produce SMCs. Measurement of marker gene

expression as well as immunostaining demonstrated that adult CPCs lacking *C-201* Exon 2 lost their ability to differentiate into SMCs (Fig. 1f-h).

CARMEN-201 induction is sufficient to trigger a SMC gene program in undifferentiated fetal CPCs

To evaluate the capacity of *C-201* to redirect fetal CPCs into the SMC lineage, we used a CRISPR-On approach. We targeted transcriptional activators (dCas9-VP64; MS2-p65-HSF1), 200 bp upstream of the *C-201* transcriptional start site (TSS) via expression of a modified gRNA containing MS2 aptamers (SAM system; [23]). Endogenous *C-201* expression was downregulated in fetal CPCs in the absence of gRNA but markedly increased when the gRNA was expressed (Fig. 2a). Compared to the large *C-201* induction, the other *CARMEN* isoforms, as well as the two hosted miRNAs, were marginally activated (Fig. 2a; Supplemental Fig. S3c). We tested therefore the effects of *C-201* manipulation on the fate of normally cardiogenic fetal CPCs. Strikingly, cells with forced *C-201* transcription produced large amount of SMCs, indicating that *C-201* expression was sufficient to adopt a SMC fate (Fig. 2b-c). Production of CMs was minimally affected, likely reflecting differentiation of untransfected fetal CPCs (Supplemental Fig. S3d-e). Globally, expression of *C-201* was found to be necessary and sufficient for inducing SMC specification in CPCs.

The *CARMEN-201* second exon contains a functional transposable element that drives SMC commitment

The results above prompted us to evaluate the role of the *C-201* second exon in SMC specification. We looked at its primary structure (397 nucleotides) and detected a short interspersed nuclear element (SINE), which was identified as a 126 nucleotide-long Mammalian-wide Interspersed Repeat (MIR)c element. Of note, the exon is highly conserved in primates but not found in other species (Fig. 2d). Intriguingly, MIRc is part of a catalog of predicted Repeat Insertion Domains of LncRNAs (RIDLS) promoting nuclear localization [18], a feature consistent with the pronounced nuclear enrichment of *C-201* (Fig. 1e). The exon also contains a partial ALU sequence.

To study the possible role of the MIRc element in determining SMC specification, we produced two lentiviral vectors for overexpressing the entire Exon 2 in fetal CPCs (Supplemental Fig. S4a). The first version contained wild-type MIRc sequences (*C-201* Ex2) whereas, in the second vector, the whole MIRc

sequence was scrambled (*C-201* mutEx2), thus maintaining length and sequence composition (Supplemental Fig. S4a). Endogenous *C-201* expression was downregulated in differentiating fetal CPCs as expected (Fig. 2e; P1). However, significant wild-type and mutated *C-201* Exon 2 expression was measured in the respective transduced groups as judged by using Exon 2-specific primers (P3). We next evaluated SMC and CM differentiation (Fig. 2f-g; Supplemental Fig. S4b-d). Non-transduced fetal CPCs differentiated into CMs. In sharp contrast, overexpression of wild-type *C-201* Exon 2 forced fetal CPCs to adopt a SMC fate, as evidenced by expression of SMC markers and immunostaining. Importantly, when the MIRc element was mutated (*C-201* mutEx2), SMC differentiation was not observed, supporting a critical role for this transposable element in the capacity of *C-201* to direct CPCs into the SMC lineage.

Identification of upstream regulators of CM and SMC specification in human CPCs

To better understand the processes leading to a switch in cell identity, we profiled the CPC transcriptomes under different experimental conditions. Principal component analysis (PCA) was conducted to evaluate differentiation when *C-201* Exon 2 was expressed and not expressed (Fig. 3a). Samples of differentiating fetal CPCs (None) revealed temporal changes (d0 / Expansion; d1; d7) characterizing CM specification. In contrast, fetal CPCs overexpressing wild-type *C-201* Exon 2 deviated significantly from the original differentiation track. Importantly, CPC samples with overexpression of the MIRc-mutated *C-201* Exon 2 were transcriptionally similar to untransfected samples, indicating again that the transposable element was necessary for SMC commitment.

We next analyzed the transcriptomic data in details (Fig. 3b; Supplemental Fig. S4e). Although fetal CPC differentiation was associated with early expression of cardiac TFs (e.g. *ISL1*; *TBX5*; *GATA4*; *NKX2-5*) and late expression of genes associated with CM excitation-contraction coupling (e.g. *MYH6*; *MYH7*; *SCN5A*; *TNNT2*), *C-201* Exon 2-overexpressing cells induced genes characterizing epicardial (e.g. *WT1*; *TCF21; TBX18*), pericyte (e.g. *ACTA2*; *PDGFRB*; *NTS5E*) and SMC lineages (e.g. *TAGLN; CNN1*; *MYH11*; *MYLK*). The two distinct transcriptomes were enriched with relevant terms in a gene ontology analysis (Supplemental Fig. S4f). Several factors characterizing the second heart field (SHF) and the outflow tract (OFT) were differentially expressed under the two experimental conditions (e.g. *GATA6*; *HAND2*; *ISL1*; *MEIS1*; *MEIS2*; *PITX2*), suggesting a developmental origin for the fetal and adult CPCs.

Interestingly, undifferentiated fetal CPCs (Expansion) expressed factors from the Iroquois family of TFs (*IRX1*; *IRX3*; *IRX4; IRX5*), which are known to be activated in mesodermal tissues, in particular the dorsal mesoderm from which the heart derives [26].

To identify regulators of specification during either CM or SMC differentiation, we took advantage of TRIAGE (Transcriptional Regulatory Inference Analysis of Gene Expression), a novel metric for inferring genes orchestrating cell identity [24]. TRIAGE is based on the observation that broad H3K27me3 occupancy at promoters enriches for genes driving cell fates. TRIAGE calculates a repressive score for each gene, which can be combined with any type of genome-wide sequencing data to predict genes governing cell differentiation. We therefore identified upstream regulators of fetal CPC specification with and without *C-201* Exon 2 overexpression, 1 and 7 days after induction of differentiation. The results of this inference analysis are presented in a way to compare rank orders based on input gene expression (right column) vs. TRIAGE ranking (left column) (Fig. 3c and d). The top ranked TRIAGE candidates revealed that key mesodermal and cardiac TFs were involved in the commitment of untransfected fetal CPCs into the CM fate whereas determinants of pericyte and SMC identity were activated following *C-201* Exon 2 expression. The complete lists of TRIAGE regulators identified under the two different experimental conditions are presented in Supplemental Table S1. Analysis of cell identity (ARCHS4; [27]) and associated biological pathways (GO BP) using all identified TRIAGE candidates validated their functional roles in CM and SMC commitment (Supplemental Fig. S5a).

To further investigate the association of *CARMEN* expression with blood vessel development in vivo, we used data reporting the comprehensive transcriptional analysis of the embryonic human heart at the single-cell level at different stages of gestation [28]. To understand how *CARMEN* expression was related to gene network changes, we performed a correlation analysis of *CARMEN* against all genes in all cells across all developmental time points (Fig. 3e). *CARMEN* abundance was associated preferentially with pericyte and SMC gene programs, and not with the expression of CM or endothelial cell markers. We next reanalyzed data generated at 6.5 weeks post-conception [28], an important point in development corresponding to the formation of the cardiac vasculature. Newly generated Uniform Manifold Approximation and Projection (UMAP) density plots revealed lineage-specific markers, reflecting the cellular diversity of the embryonic human heart including epicardial cells (*WT1*; *TCF21*; *TBX18*), pericytes

(*MCAM*; *CSPG4*; *ACTA2*; *PDGFRB*), and SMCs (*GATA6*; *TAGLN*; *CNN1*; *MYH11*) (Fig. 3f). *CARMEN* was found expressed preferentially in these cells, substantiating an important role for this locus in pericyte and SMC specification from the epicardium during development of the human heart. In contrast, CMs and endothelial cells, marked by *TBX5*; *GATA4*; *NKX2-5*; *MYH6* and *PECAM*; *KDR*, did not expressed *CARMEN* at this developmental stage (Supplemental Fig. S5b). Interestingly, *ALDH1A2* and the COUP transcription factor *NR2F2*, critical for atrial identity, were also expressed in *CARMEN*-expressing cells.

The MIRc element is a binding module for the RE1 Silencing Transcription Factor

Many lncRNAs function through interacting with proteins. To identify *C-201* protein partners, we performed a RNA pulldown assay. Biotinylated *C-201* Exon 2 was used as a bait to purify *C-201*-associated proteins from adult CPC lysates. As control, we used a mutated *C-201* Exon 2 lacking the MIRc element. Proteins were identified by mass spectrometry. Three proteins were detected as significantly associated to *C-201* Exon 2, namely the transcriptional repressor RE1 Silencing Transcription Factor (REST; aka Neuron Restrictive Silencer Factor), the RNA methyltransferase NOP2/Sun RNA Methyltransferase 6 (NSUN6), and the Replication Protein A1 (RPA1), a protein implicated in stabilization of single-stranded DNA (Supplemental Fig. S6a; Supplemental Table S2). We first confirmed the association of each protein with *C-201* by pulling down the full *C-201* transcript and quantifying the amount of bound proteins by Western blotting (Fig. 4a-c; see full unedited gels in Supplementary Information). An antisense *C-201* transcript was used as control. The results demonstrated the specific interaction of *C-201* with REST, NSUN6 and RPA1 in proliferating and differentiating adult CPCs. We next performed a RNA immunoprecipitation assay (RIP) using antibodies directed against REST, NSUN6 and RPA1 respectively (Fig. 4d-f). Quantitative measurement of bound *CARMEN* isoforms confirmed the interaction of *C-201* with REST, NSUN6 and RPA1 during CPC expansion and differentiation. No other *CARMEN* isoforms were found associated to REST (Supplemental Fig. S6b). In contrast, small amounts of *C-205* were detected as bound to NSUN6, and *C-217* appeared to interact with both NSUN6 and RPA1 (Supplemental Fig. S6c-d). Finally, to determine whether REST possessed intrinsic propensity to bind MIRc-containing transcripts, we performed a REST RIP coupled to RNA profiling. REST-bound transcripts were found significantly enriched in sequences containing a MIRc element as compared to transcripts not

bound by REST with similar length distribution and orientation. Nevertheless, the enrichment is also higher when exploring repeat-containing genes in general, suggesting that global REST binding to RNA molecules could require additional transposable elements (Supplemental Fig. S6e; Supplemental Table S3).

To evaluate the role of REST in *C-201*-mediated CPC specification, we first used a knockdown approach. Fetal CPCs were transfected with control or REST siRNA, and induced to differentiate into SMC following *C-201* Exon 2 overexpression (Fig. 4g-h). Under control conditions, *C-201* Exon 2 expression forced CPCs to adopt a SMC specification. In sharp contrast, REST knockdown abolished the capacity of *C-201*-expressing CPCs to commit to the SMC lineage. To confirm these results, we tested the effects of REST silencing in adult CPCs spontaneously differentiating into SMC (Supplemental Fig. S6f). Again, in the absence of REST, adult CPCs were unable to produce a SMC progeny. Interestingly, *C-201* appeared downregulated in differentiating REST-deficient CPCs. This was also confirmed using RNA BaseScope in situ hybridization in adult CPCs (Supplemental Fig. S6g). The resetting of *C-201* expression following REST knockdown mimicked therefore what observed in differentiating fetal CPCs (Supplemental Fig. S1a-b). Moreover, the cellular distribution of the *C-201* isoform was modified following REST silencing (Supplemental Fig. S6h). Significant cytoplasmic enrichment was evident in the absence of REST, in contrast to what measured under basal conditions. This observation suggested therefore that REST, which carries a nuclear localization signal, might contribute to retain *C-201* in the nucleus via its capacity to bind the MIRc element in the second exon.

CARMEN-201 inhibits the CM fate via REST-mediated repression of cardiogenic transcription factor expression

The association of *C-201* with REST suggested a mechanism involving the targeting of the repressor to important regulatory loci to control cell fate in differentiating CPCs. In addition, RPA1, a *C-201* protein partner, has been implicated in RNA:DNA triple helix stabilization [29], indicating that *C-201* could interact with DNA sequences at target promoters. Thus, we took advantage of Triplex Domain Finder (TDF), an application developed to detect DNA binding domains (DBDs) in lncRNAs [30]. TDF identifies also the DNA regions bound by the selected lncRNAs, i.e. gene promoters containing binding

sites for the lncRNA DBDs. Because REST had been associated with repression, we sought to identify *C-201* target promoters within the list of downregulated genes following *C-201* Exon 2 overexpression. Several DBDs were predicted in *C-201*, in particular in the sequences spanning the second exon (Fig. 5a). As control, we performed a similar analysis for *C-205* and *C-217*. The *C-205* transcript was found to contain distinct DBDs (Fig. 5a) whereas *C-217* was not predicted to contain significant DBDs (not shown). In total, 447 gene promoters were identified as potentially bound by *C-201*, and 387 by *C-205* respectively. Among those, 337 were uniquely associated with *C-201*. These genes were related to GO Biological Processes defining striated muscle contraction (Fig. 5b). In order to identify relevant targets of *C-201*/REST action, we crossed the list of *C-201*-bound genes as predicted by TDF with the list of TRIAGE candidates and the list of validated cardiac genes (Human Protein Atlas - ENSEMBL) (Fig. 5c; Supplemental Table S4). Hypergeometric tests explored the significance of the overlaps and revealed four primary candidates: *IRX1*; *IRX5*; *ISL1* and *SFRP1*. ISL1 is a member of the LIM homeodomain family of transcription factor, crucial for the development of the SHF. The two Iroquois homeobox transcription factors IRX1 and IRX5 have been involved in developmental patterning in the embryonic heart. Finally, SFRP1 is a modulator of the WNT pathway that plays important roles in cardiac specification and differentiation. Importantly, single-cell analysis demonstrated that these factors were not expressed in *CARMEN*-expressing cells in the embryonic human heart at 6.5 weeks of gestation (Supplemental Fig. S5b). Importantly, all four genes contained REST binding sites as determined by chromatin immunoprecipitation followed by sequencing (ChIP-Seq) in a study interrogating REST binding in various cell types (Supplemental Fig. S7a; Gene Expression Omnibus: GSM803369; GSM1010735; GSM1010804) [31]. We evaluated therefore REST occupancy at the promoters of *IRX1*, *IRX5*, *ISL1* and *SFRP1* in differentiating fetal and adult CPCs by ChIP-quantitative real-time (q)PCR. As expected, REST occupied the promoter of the different candidate gene solely in adult CPCs expressing *C-201*, and not in fetal CPCs (Supplemental Fig. S7b). In these experiments, we used *GAPDH* as a negative control (REST occupancy in neither fetal nor adult CPCs) and *SYN1* as a positive control (REST occupancy in both fetal and adult CPCs). Then, to formally demonstrate the dependence of REST targeting to *IRX1*; *IRX5*; *ISL1* and *SFRP1* on *C-201* action, we performed an additional experiment in adult CPCs with or without *C-201*

silencing. Consistently, REST occupancy at candidate promoters in adult CPCs was blunted following GapmeR-mediated *C-201* knockdown (Figure 5d).

To validate the relevance of *ISL1*, *IRX1*, *IRX5* and *SFRP1* in CPC specification, we first determined expression in fetal CPCs induced to differentiate into SMC following forced *C-201* expression using CRISPR-On (Fig. 5e). Each candidate was downregulated after induction of *C-201* expression. We then measured expression in adult CPC clones lacking *C-201* exon 2 (Δ201Ex2), i.e. not able to activate a SMC gene program. *ISL1*, *IRX1*, *IRX5* and *SFRP1* expression was restored in these cells during differentiation as compared to what observed in wild-type cells (Fig. 5f). Furthermore, we evaluated expression after manipulating REST. We observed re-expression of the four factors in differentiating adult CPCs after REST knockdown (Supplemental Fig. S7c). Moreover, REST silencing allowed also re-expression of *ISL1*, *IRX1*, *IRX5* and *SFRP1* in fetal CPCs overexpressing *C-201* Exon 2 (Fig. 5g). Altogether, these findings supported that the four candidates were under control by *C-201* via REST-mediated repression.

ISL1, *IRX1*, *IRX5* and *SFRP1* silencing promotes the SMC fate

We next proceeded to validate the importance of *ISL1*, *IRX1*, *IRX5* and *SFRP1* in controlling specification into the CM vs. the SMC lineage. To mimic REST-mediated repression, we used a siRNA approach to knockdown each candidate in fetal CPCs normally committing to the CM lineage. We first evaluated the effects of individual factor silencing on the capacity of fetal CPCs to produce a functional progeny. Knocking down either *IRX1*, *IRX5* or *SFRP1* did not affect other candidate gene expression but *ISL1* knockdown slightly decreased *IRX1*, *IRX5* and *SFRP1* levels (Supplemental Fig. S8a-d), suggesting *ISL1* lies upstream of these factors in the cardiac regulatory network, in accordance with its role as a pioneer transcription factor in the developing heart [32]. We then investigated re-specification of fetal CPCs into the SMC fate following siRNA-mediated silencing of each factor individually or in combination. In differentiating fetal CPCs, knocking down either *IRX1*, *IRX5*, *ISL1* or *SFRP1* restored epicardial gene expression, i.e. *WT1*, *TCF21* and *TBX18*, confirming that downregulation of these critical cardiogenic factors was a mandatory step in reprogramming CPCs into the smooth muscle fate (Fig. 6a-d). In addition, individual factor silencing also resulted in the reexpression of *GATA6*, *HAND2*, *PDGFRA* and *TBX20*,

(Supplemental Fig. S8e-h), which are known to mark bipotential cardiac precursors giving raise to CMs and SMCs [33]. Nevertheless, manipulating each candidates separately has little impact on SMC gene expression (Supplemental Fig. S8i-l). In fact, *ISL1* knockdown had even a negative effect on late SMC maker expression. This suggested that *ISL1* operated at the onset of CPC specification but was also necessary for late-stage differentiation.

We tested therefore combinations of siRNAs targeting *IRX1*, *IRX5* and *SFRP1* (Fig. 6e). As a positive control for the activation of the SMC gene program, *C-201* Exon 2-overexpressing fetal CPCs were included in the experiment. Each combination was associated with a large induction of epicardial and SMC gene expression as compared to individual knockdown, with maximal impact achieved when all three factors were downregulated simultaneously. This manipulation was as potent as *C-201* Exon 2 overexpression in inducing SMC genes in normally cardiogenic CPCs. Accordingly, massive SMC differentiation was observed by immunostaining following *IRX1*, *IRX5* and *SFRP1* knockdown (Fig. 6f). Interestingly, commitment occurred at the expense of the cardiogenic lineage (Fig. 6e and f) but had no impact on endothelial cell production (not shown). Our data indicated therefore that *IRX1*, *IRX5* and *SFRP1* downregulation was sufficient to redirect fetal CPCs into the epicardial and the SMC lineages. Nevertheless, as mentioned above, *ISL1* expression appeared necessary during SMC differentiation. To formally demonstrate this point, we performed an additional experiment in which the four factors were silenced together (Supplemental Fig. S8m). In this case, *ISL1* silencing produced a slight negative effect on SMC marker expression induced by combined *IRX1*, *IRX5* and *SFRP*1 knockdown, sustaining a role for *ISL1* in the late stage of SMC differentiation.

Interestingly, manipulating *IRX1*, *IRX5* or *SFRP1* had a striking effect on *CARMEN* isoform expression (Fig. 6g). Indeed, while endogenous *C-201* was downregulated during specification in differentiating fetal CPCs, its expression was reactivated after *IRX5* and *SFRP1* knockdown, and even more so when *IRX5* and *SFRP1* were silenced together, suggesting *C-201* was negatively regulated by the two cardiogenic factors. Remarkably, *C-217* expression demonstrated a mirror image, consistent with coordinated regulation of the two isoforms and suggesting a switch might operate during SMC specification. *C-205* was not modulated under these different conditions.

CARMEN-201 expression is increased in response to myocardial infarction in humans

In an attempt to evaluate the relevance of our findings in disease, we queried the association of *CARMEN* with cardiovascular traits using CTG-VIEW (https://view.genoma.io). We identified important phenotypes related to cardiovascular conditions as strongly associated with *CARMEN* (Fig. 7a). This prompted us to investigate whether *C-201* was differentially expressed in the damaged myocardium. We first used RNA BaseScope in situ hybridization to localize *C-201* expression in the human heart. Samples were collected from explanted hearts of transplant patients, and expression was compared in CMs vs. mural cells (Fig. 7b-e). *C-201* was found uniquely expressed in mural cells of large coronary vessels. Immunostaining for VIMENTIN (marking endothelial cells and fibroblasts) and smooth-muscle myosin heavy chain (SMMHC; marking SMCs) supported *C-201* expression being associated primarily with SMCs (Fig. 7f; Supplemental Fig. S8n). *C-201* expression seemed equally distributed in the ventricular and atrial vasculature. Next, we measured *C-201* expression in the blood of patients experiencing acute coronary syndrome, with no prior history of cardiac disease. Plasma samples were obtained during angioplasty that took place less than 1 hours after myocardial infarction, and at 24 and 48 hours thereafter (Figure 7g). Individuals were classified based on the presence or absence of ST elevation, namely STEMI and non-STEMI (NSTEMI). *C-201* was not expressed immediately after infarction, suggesting that the transcript was not induced under basal conditions. However, the amounts of transcript dramatically increased after one and two days. Importantly, circulating *C-201* concentrations were more elevated in STEMI vs. non-STEMI patients. Altogether, it suggested that *C-201* was expressed in large vessels of the heart and responded acutely to hemodynamic stress with an expression being proportional to the severity of the disease.

DISCUSSION

In this study, we characterized for the first time the role of lncRNA isoforms in cell fate determination through a systematic examination of the human *CARMEN* locus. In primary human CPCs committing to the SMC lineage, the *C-201* isoform associates with REST via its MIRc element, targets the repressor to important cardiogenic loci, namely *IRX1*, *IRX5*, *SFRP1* and *ISL1*, represses their expression

and promotes SMC specification (see Graphical Abstract). Conversely, in CPCs adopting a CM fate, *C-201* is not expressed, allowing *IRX1*, *IRX5*, *ISL1* and *SFRP1* expression and the subsequent activation of the cardiogenic program. Importantly, the MIRc-containing exon in *C-201* is found in primates but not in other mammals, suggesting that MIRc-mediated functions controlling commitment into the SMC lineage has been integrated in the *CARMEN* locus only recently in evolution. The *CARMEN* locus has been involved in cardiogenesis, implicating however other isoforms than *C-201* [21]. Our data suggest that coordinate regulation of *C-201* and *C-217* expression takes place during specification, providing a plausible mechanism for controlling specification. *CARMEN* isoforms appear to share a single promoter. Yet, additional transcription start sites have been recently detected in the *C-201* isoform, suggesting transcriptional regulation might control *C-201* expression in differentiating SMCs [34].

Multipotent cardiovascular precursor cells expressing *ISL1* give rise to both CMs and SMCs [2-4]. In this context, our TRIAGE analysis identifies key cardiac TFs as regulators of fetal CPC differentiation. On the other hand, CPCs respecified into the SMC lineage after *C-201* Exon 2 overexpression express a different gene program. Induction of *GATA6*, *HAND2, PDGFRA* and *TBX20* in CPCs is a characteristic feature of cardiovascular intermediates capable of producing CMs and SMCs [33]. We show also that commitment to the SMC lineage is characterized by the stepwise expression of markers of epicardium-derived cells (EPDCs) such as *WT1*, *MEOX1*, *KRT19* and *TBX18*, and pericytes such as *MCAM*, *CSPG4*, *ACTA2* and *PDGFRB*. During development, EPDCs establish the subepicardial mesenchyme, then migrate into the myocardium. These cells represent a known source of pericytes and SMCs for the forming coronary vasculature [35]. In addition, genetic tracing experiments suggest that epicardial cells can also give rise to a myocardial progeny [36-38]. Along the same line, a recent single-cell analysis identifies the juxta-cardiac field (JCF) contributing to both EPDCs and CMs [39]. Trajectory analysis revealed a link between precursors from the JCF and the posterior SHF, supporting the postulated developmental origin of *CARMEN*-expressing CPCs. Of note, TRIAGE identifies *IRX1* and *IRX5* as important regulators of cardiogenesis. *IRX1* is detected in the trabeculated and compact myocardium of the developing ventricular septum whereas *IRX5* demonstrates a subendocardial to subepicardial gradient of expression [40]. Consistently, our experiments show that knocking down *IRX1* and *IRX5* in fetal CPCs allows reexpression of epicardial and SMC markers, suggesting expression of the two factors is sufficient to

maintain a cardiogenic identity in committed precursors. *C-201* targets also *SFRP1*, a known WNT antagonist. Downregulation of the WNT pathway is an important step in establishing cardiac fates [41].

In specifying CPCs, *C-201* acts via REST-mediated repression. A role for *C-201* in blocking REST activity during SMC determination, for instance via sequestering REST, is unlikely since REST silencing abolishes SMC commitment in *C*-201-expressing CPCs. Consistently, REST acts as a transcriptional repressor in the developing heart, where it is thought to repress adult cardiac gene expression [42-44]. Accordingly, blockade of REST in the heart leads to cardiac dysfunction [45]. In addition, our results suggest that temporal REST expression during the development of the heart also reflects the role of REST in cell fate determination. REST binds *C-201* but not *C-205* and *C-217*, further substantiating the importance of the *C-201*/REST complex for SMC differentiation. *C-201* appears to be also indirectly under control by REST. *C-201* relocalizes into the cytoplasm upon REST silencing. Therefore, the nuclear enrichment of *C-201* could depend in part on its binding to REST. In this vein, REST binds *C-201* via the MIRc repeat in the second exon, which was recently demonstrated to be associated with transcript nuclear localization [18].

Then, *C-201* associates with NSUN6 and RPA1. A recent study demonstrated a role for NSUN6 in methylating mRNAs and lncRNAs, such as *MALAT1*, *NEAT1* AND *XIST* [46]. Mechanistically, lncRNA m5C modification could be involved in transcript structure and stability [47]. *C-201* associates also to RPA1. Importantly, RPA1 binds RNA with high affinity and promotes R-loop formation with homologous DNA [29]. RNA-DNA hybrids initiate cellular processes regulating transcription and genome dynamics, two important determinants of cell specification [48, 49]. Thus, RPA1 might contribute to effective targeting of REST at regulatory loci via its capacity to stabilize *C-201*/promoter association, a feature consistent with the predicted DNA binding domains in *C-201*.

CARMEN is expressed in adult tissues, particularly in the heart and the vasculature, reflecting expression in CMs and SMCs [50]. An increasing body of evidence suggests *CARMEN* is associated with pathological states in the cardiovascular system [22]. Relevant to the present work, *CARMEN* was recently demonstrated to regulate SMC differentiation and proliferation in atherosclerotic plaques [34]. Unstable regions, in which high proliferation of dedifferentiated SMCs is observed, were characterized with decreased *CARMEN* levels. Consistently, SMCs adopting a synthetic phenotype characterized *Carmen* knockout mice. We have demonstrated previously that *CARMEN* is induced in the stressed mouse and

human hearts [21]. Interestingly, human *CARMEN* isoforms were found differentially expressed depending on the cardiac pathology, exemplifying again the complexity of the regulation of the *CARMEN* locus. Here, we show that *C-201* levels increase in the blood during the acute phase of myocardial infarction. The likely source of circulating *C-201* is the damaged heart. However, we cannot rule out the possibility that hemodynamic stress also stimulates release from the peripheral vasculature. Nevertheless, assuming a cardiac origin for *C-201*, its expression in CPCs could be part of the healing process initiated following injury. In this scenario, CPCs expressing *C-201* would be specified preferentially into the SMC lineage. Increased myocardial tissue perfusion has been reported in cell-based regenerative therapies for heart disease. However, clinical trials failed to demonstrate functional improvement. This can be expected if precursors are diverted from the cardiogenic lineage secondary to *C-201* expression. Our data propose therefore a mean to improve CM production via modulating *C-201* expression in cardiac precursors. Finally, *C-201* could represent an interesting biomarker for assessing the extent of cardiovascular damage in various pathological situations.

Altogether, this work demonstrates how a biological switch is encoded in lncRNA sequence to regulate cardiovascular specification. We have linked two key phenomena, namely alternative splicing and the presence of deeply-conserved transposable elements. LncRNAs display far greater levels of alternative splicing, although it has not been clear whether this reflects relaxed constraint or regulated production of isoforms with distinct functions [25]. Here, we have shown an example where these two processes converge to produce functional transcript isoforms, and provided the first physiological role for a transposable element acting via a lncRNA during heart development.

FUNDING

This work was supported by grants from the Swiss National Science Foundation (T.P.; Grant No. CRSII5-1_173738 and 31003A_182322).

AUTHORS CONTRIBUTION

T.P. conceived the project, designed experiments and wrote the paper. I.S. designed and performed all wet-lab experiments, with help from M.N., P.A. and F.A.. P.C. and R.J. conducted the bioinformatic analyses. Y.S., S.S., W.J.S. and N.P. performed the TRIAGE, GWAS and single-cell analyses. F.R. provided critical human material for RNA FISH experiment, and her expertise in heart development.

ACKNOWLEDGEMENTS

We express our gratitude to Dr Gabriel Cuellar Partida, University of Queensland, Brisbane, Australia, for his help in analyzing the GWAS data. We are grateful to Dr Nicole Deglon and Dr Maria Del Rey, University of Lausanne Medical School, Switzerland, for the plasmids used to prepare lentiviral vectors. We thank the Genomic Technologies Facility, the Protein Analysis Facility, the Cellular Imaging Facility and the Mouse Pathology Facility at the University of Lausanne, Switzerland, for providing expertise in transcriptomics, proteomics, imaging and histology respectively.

CONFLICT OF INTEREST

T.P. is co-founder of Haya Therapeutics, Epalinges, Switzerland

DATA AVAILABILITY

All transcriptomic data has been deposited to GEO with the identifier GSE199930.

REFERENCES

1. Meilhac SM, Buckingham ME. The deployment of cell lineages that form the mammalian heart. *Nat Rev Cardiol* 2018;**15**:705-724.
2. Kattman SJ, Huber TL, Keller GM. Multipotent flk-1+ cardiovascular progenitor cells give rise to the cardiomyocyte, endothelial, and vascular smooth muscle lineages. *Dev Cell* 2006;**11**:723-732.
3. Moretti A, Caron L, Nakano A, Lam JT, Bernshausen A, Chen Y, Qyang Y, Bu L, Sasaki M, Martin-Puig S, Sun Y, Evans SM, Laugwitz KL, Chien KR. Multipotent embryonic isl1+ progenitor cells lead to cardiac, smooth muscle, and endothelial cell diversification. *Cell* 2006;**127**:1151-1165.
4. Wu SM, Fujiwara Y, Cibulsky SM, Clapham DE, Lien CL, Schultheiss TM, Orkin SH. Developmental origin of a bipotential myocardial and smooth muscle cell precursor in the mammalian heart. *Cell* 2006;**127**:1137-1150.
5. Gonzales C, Ullrich ND, Gerber S, Berthonneche C, Niggli E, Pedrazzini T. Isolation of cardiovascular precursor cells from the human fetal heart. *Tissue Eng Part A* 2012;**18**:198-207.
6. Plaisance I, Perruchoud S, Fernandez-Tenorio M, Gonzales C, Ounzain S, Ruchat P, Nemir M, Niggli E, Pedrazzini T. Cardiomyocyte lineage specification in adult human cardiac precursor cells via modulation of enhancer-associated long noncoding RNA expression. *JACC BST* 2016;**1**:472-493.
7. Uszczynska-Ratajczak B, Lagarde J, Frankish A, Guigo R, Johnson R. Towards a complete map of the human long non-coding RNA transcriptome. *Nat Rev Genet* 2018;**19**:535-548.
8. Gil N, Ulitsky I. Regulation of gene expression by cis-acting long non-coding RNAs. *Nat Rev Genet* 2020;**21**:102-117.
9. Quinn JJ, Chang HY. Unique features of long non-coding RNA biogenesis and function. *Nat Rev Genet* 2016;**17**:47-62.
10. Klattenhoff CA, Scheuermann JC, Surface LE, Bradley RK, Fields PA, Steinhauser ML, Ding H, Butty VL, Torrey L, Haas S. Braveheart, a long noncoding RNA required for cardiovascular lineage commitment. *Cell* 2013;**152**:570-583.

11. Grote P, Wittler L, Hendrix D, Koch F, Währisch S, Beisaw A, Macura K, Bläss G, Kellis M, Werber M. The tissue-specific lncRNA Fendrr is an essential regulator of heart and body wall development in the mouse. *Dev Cell* 2013;**24**:206-214.

12. Alexanian M, Maric D, Jenkinson SP, Mina M, Friedman CE, Ting CC, Micheletti R, Plaisance I, Nemir M, Maison D, Kernen J, Pezzuto I, Villeneuve D, Burdet F, Ibberson M, Leib SL, Palpant NJ, Hernandez N, Ounzain S, Pedrazzini T. A transcribed enhancer dictates mesendoderm specification in pluripotency. *Nat Commun* 2017;**8**:1806.

13. Han P, Li W, Lin CH, Yang J, Shang C, Nurnberg ST, Jin KK, Xu W, Lin CY, Lin CJ, Xiong Y, Chien HC, Zhou B, Ashley E, Bernstein D, Chen PS, Chen HS, Quertermous T, Chang CP. A long noncoding RNA protects the heart from pathological hypertrophy. *Nature* 2014;**514**:102-106.

14. Micheletti R, Plaisance I, Abraham BJ, Sarre A, Ting CC, Alexanian M, Maric D, Maison D, Nemir M, Young RA, Schroen B, Gonzalez A, Ounzain S, Pedrazzini T. The long noncoding RNA Wisper controls cardiac fibrosis and remodeling. *Sci Transl Med* 2017;**9**.

15. Bell RD, Long X, Lin M, Bergmann JH, Nanda V, Cowan SL, Zhou Q, Han Y, Spector DL, Zheng D, Miano JM. Identification and initial functional characterization of a human vascular cell-enriched long noncoding RNA. *Arterioscler Thromb Vasc Biol* 2014;**34**:1249-1259.

16. Ballantyne MD, Pinel K, Dakin R, Vesey AT, Diver L, Mackenzie R, Garcia R, Welsh P, Sattar N, Hamilton G, Joshi N, Dweck MR, Miano JM, McBride MW, Newby DE, McDonald RA, Baker AH. Smooth Muscle Enriched Long Noncoding RNA (SMILR) Regulates Cell Proliferation. *Circulation* 2016;**133**:2050-2065.

17. Kirk JM, Kim SO, Inoue K, Smola MJ, Lee DM, Schertzer MD, Wooten JS, Baker AR, Sprague D, Collins DW, Horning CR, Wang S, Chen Q, Weeks KM, Mucha PJ, Calabrese JM. Functional classification of long non-coding RNAs by k-mer content. *Nat Genet* 2018;**50**:1474-1482.

18. Carlevaro-Fita J, Polidori T, Das M, Navarro C, Zoller TI, Johnson R. Ancient exapted transposable elements promote nuclear enrichment of human long noncoding RNAs. *Genome Res* 2019;**29**:208-222.

19. Kapusta A, Kronenberg Z, Lynch VJ, Zhuo X, Ramsay L, Bourque G, Yandell M, Feschotte C. Transposable elements are major contributors to the origin, diversification, and regulation of vertebrate long noncoding RNAs. *PLoS Genet* 2013;**9**:e1003470.

20. Ziegler C, Kretz M. The More the Merrier-Complexity in Long Non-Coding RNA Loci. *Front Endocrinol (Lausanne)* 2017;**8**:90.

21. Ounzain S, Micheletti R, Arnan C, Plaisance I, Cecchi D, Schroen B, Reverter F, Alexanian M, Gonzales C, Ng SY, Bussotti G, Pezzuto I, Notredame C, Heymans S, Guigo R, Johnson R, Pedrazzini T. CARMEN, a human super enhancer-associated long noncoding RNA controlling cardiac specification, differentiation and homeostasis. *J Mol Cell Cardiol* 2015;**89**:98-112.

22. Vacante F, Denby L, Sluimer JC, Baker AH. The function of miR-143, miR-145 and the MiR-143 host gene in cardiovascular development and disease. *Vascul Pharmacol* 2019;**112**:24-30.

23. Konermann S, Brigham MD, Trevino AE, Joung J, Abudayyeh OO, Barcena C, Hsu PD, Habib N, Gootenberg JS, Nishimasu H, Nureki O, Zhang F. Genome-scale transcriptional activation by an engineered CRISPR-Cas9 complex. *Nature* 2015;**517**:583-588.

24. Shim WJ, Sinniah E, Xu J, Vitrinel B, Alexanian M, Andreoletti G, Shen S, Sun Y, Balderson B, Boix C, Peng G, Jing N, Wang Y, Kellis M, Tam PPL, Smith A, Piper M, Christiaen L, Nguyen Q, Boden M, Palpant NJ. Conserved Epigenetic Regulatory Logic Infers Genes Governing Cell Identity. *Cell Syst* 2020;**11**:625-639 e613.

25. Lagarde J, Johnson R. Capturing a Long Look at Our Genetic Library. *Cell Syst* 2018;**6**:153-155.

26. Christoffels VM, Keijser AG, Houweling AC, Clout DE, Moorman AF. Patterning the embryonic heart: identification of five mouse Iroquois homeobox genes in the developing heart. *Dev Biol* 2000;**224**:263-274.

27. Lachmann A, Torre D, Keenan AB, Jagodnik KM, Lee HJ, Wang L, Silverstein MC, Ma'ayan A. Massive mining of publicly available RNA-seq data from human and mouse. *Nat Commun* 2018;**9**:1366.

28. Asp M, Giacomello S, Larsson L, Wu C, Furth D, Qian X, Wardell E, Custodio J, Reimegard J, Salmen F, Osterholm C, Stahl PL, Sundstrom E, Akesson E, Bergmann O, Bienko M, Mansson-

Broberg A, Nilsson M, Sylven C, Lundeberg J. A Spatiotemporal Organ-Wide Gene Expression and Cell Atlas of the Developing Human Heart. *Cell* 2019;**179**:1647-1660 e1619.

29. Mazina OM, Somarowthu S, Kadyrova LY, Baranovskiy AG, Tahirov TH, Kadyrov FA, Mazin AV. Replication protein A binds RNA and promotes R-loop formation. *J Biol Chem* 2020;**295**:14203-14213.

30. Kuo CC, Hanzelmann S, Senturk Cetin N, Frank S, Zajzon B, Derks JP, Akhade VS, Ahuja G, Kanduri C, Grummt I, Kurian L, Costa IG. Detection of RNA-DNA binding sites in long noncoding RNAs. *Nucleic Acids Res* 2019;**47**:e32.

31. Rockowitz S, Lien WH, Pedrosa E, Wei G, Lin M, Zhao K, Lachman HM, Fuchs E, Zheng D. Comparison of REST cistromes across human cell types reveals common and context-specific functions. *PLoS Comput Biol* 2014;**10**:e1003671.

32. Gao R, Liang X, Cheedipudi S, Cordero J, Jiang X, Zhang Q, Caputo L, Gunther S, Kuenne C, Ren Y, Bhattacharya S, Yuan X, Barreto G, Chen Y, Braun T, Evans SM, Sun Y, Dobreva G. Pioneering function of Isl1 in the epigenetic control of cardiomyocyte cell fate. *Cell Res* 2019;**29**:486-501.

33. Noseda M, Harada M, McSweeney S, Leja T, Belian E, Stuckey DJ, Abreu Paiva MS, Habib J, Macaulay I, de Smith AJ, al-Beidh F, Sampson R, Lumbers RT, Rao P, Harding SE, Blakemore AI, Jacobsen SE, Barahona M, Schneider MD. PDGFRalpha demarcates the cardiogenic clonogenic Sca1+ stem/progenitor cell in adult murine myocardium. *Nat Commun* 2015;**6**:6930.

34. Vacante F, Rodor J, Lalwani MK, Mahmoud AD, Bennett M, De Pace AL, Miller E, Van Kuijk K, de Bruijn J, Gijbels M, Williams TC, Clark MB, Scanlon JP, Doran AC, Montgomery R, Newby DE, Giacca M, O'Carroll D, Hadoke PWF, Denby L, Sluimer JC, Baker AH. CARMN Loss Regulates Smooth Muscle Cells and Accelerates Atherosclerosis in Mice. *Circ Res* 2021;**128**:1258-1275.

35. Quijada P, Trembley MA, Small EM. The Role of the Epicardium During Heart Development and Repair. *Circ Res* 2020;**126**:377-394.

36. Cai CL, Martin JC, Sun Y, Cui L, Wang L, Ouyang K, Yang L, Bu L, Liang X, Zhang X, Stallcup WB, Denton CP, McCulloch A, Chen J, Evans SM. A myocardial lineage derives from Tbx18 epicardial cells. *Nature* 2008;**454**:104-108.

37. Zhou B, Ma Q, Rajagopal S, Wu SM, Domian I, Rivera-Feliciano J, Jiang D, von Gise A, Ikeda S, Chien KR, Pu WT. Epicardial progenitors contribute to the cardiomyocyte lineage in the developing heart. *Nature* 2008;**454**:109-113.

38. Lescroart F, Chabab S, Lin X, Rulands S, Paulissen C, Rodolosse A, Auer H, Achouri Y, Dubois C, Bondue A, Simons BD, Blanpain C. Early lineage restriction in temporally distinct populations of Mesp1 progenitors during mammalian heart development. *Nat Cell Biol* 2014;**16**:829-840.

39. Tyser RCV, Ibarra-Soria X, McDole K, Arcot Jayaram S, Godwin J, van den Brand TAH, Miranda AMA, Scialdone A, Keller PJ, Marioni JC, Srinivas S. Characterization of a common progenitor pool of the epicardium and myocardium. *Science* 2021;**371**.

40. Kim KH, Rosen A, Bruneau BG, Hui CC, Backx PH. Iroquois homeodomain transcription factors in heart development and function. *Circ Res* 2012;**110**:1513-1524.

41. Protze SI, Lee JH, Keller GM. Human Pluripotent Stem Cell-Derived Cardiovascular Cells: From Developmental Biology to Therapeutic Applications. *Cell Stem Cell* 2019;**25**:311-327.

42. Kuwahara K, Saito Y, Takano M, Arai Y, Yasuno S, Nakagawa Y, Takahashi N, Adachi Y, Takemura G, Horie M, Miyamoto Y, Morisaki T, Kuratomi S, Noma A, Fujiwara H, Yoshimasa Y, Kinoshita H, Kawakami R, Kishimoto I, Nakanishi M, Usami S, Saito Y, Harada M, Nakao K. NRSF regulates the fetal cardiac gene program and maintains normal cardiac structure and function. *EMBO J* 2003;**22**:6310-6321.

43. Zhang D, Wu B, Wang P, Wang Y, Lu P, Nechiporuk T, Floss T, Greally JM, Zheng D, Zhou B. Non-CpG methylation by DNMT3B facilitates REST binding and gene silencing in developing mouse hearts. *Nucleic Acids Res* 2017;**45**:3102-3115.

44. Bingham AJ, Ooi L, Kozera L, White E, Wood IC. The repressor element 1-silencing transcription factor regulates heart-specific gene expression using multiple chromatin-modifying complexes. *Mol Cell Biol* 2007;**27**:4082-4092.

45. Kuwahara K. Role of NRSF/REST in the regulation of cardiac gene expression and function. *Circ J* 2013;**77**:2682-2686.

46. Selmi T, Hussain S, Dietmann S, Heiss M, Borland K, Flad S, Carter JM, Dennison R, Huang YL, Kellner S, Bornelov S, Frye M. Sequence- and structure-specific cytosine-5 mRNA methylation by NSUN6. *Nucleic Acids Res* 2021;**49**:1006-1022.

47. Huang T, Chen W, Liu J, Gu N, Zhang R. Genome-wide identification of mRNA 5-methylcytosine in mammals. *Nat Struct Mol Biol* 2019;**26**:380-388.

48. Aguilera A, Garcia-Muse T. R loops: from transcription byproducts to threats to genome stability. *Mol Cell* 2012;**46**:115-124.

49. Santos-Pereira JM, Aguilera A. R loops: new modulators of genome dynamics and function. *Nat Rev Genet* 2015;**16**:583-597.

50. Papatheodorou I, Moreno P, Manning J, Fuentes AM, George N, Fexova S, Fonseca NA, Fullgrabe A, Green M, Huang N, Huerta L, Iqbal H, Jianu M, Mohammed S, Zhao L, Jarnuczak AF, Jupp S, Marioni J, Meyer K, Petryszak R, Prada Medina CA, Talavera-Lopez C, Teichmann S, Vizcaino JA, Brazma A. Expression Atlas update: from tissues to single cells. *Nucleic Acids Res* 2020;**48**:D77-D83.

FIGURE LEGENDS

Figure 1. *CARMEN-201* controls SMC specification via its second exon

(a-b) Representative images and quantification of ACTN2-positive TNNI-positive CMs and SMMHC-positive SMCs in differentiating fetal and adult CPC cultures. Scale bar: 50 µm. (c) Annotated *CARMEN* isoforms. The *CARMEN-201* second exon is highlighted in red. (d) Absolute quantification of *CARMEN-201 (C-201)*, *CARMEN-205 (C-205)* and *CARMEN-217 (C-217)* in differentiating fetal and adult CPCs. (e) Nuclear and cytoplasmic levels of *CARMEN-201*, *CARMEN-205*, *CARMEN-217, ACTB*, and *NEAT*. (f) Expression of *CARMEN-201*, *CARMEN-205*, *CARMEN-217*, SMC markers (*MYH11*; *CNN1*; *TAGLN*), and CM markers (*MYH6*; *MYH7*) in adult WT and ∆201Ex2 CPC clones lacking *CARMEN-201* Exon 2. (g-h) Representative images and quantification of SMMHC-positive CNN1-positive TAGLN-positive SMCs in cultures of differentiating adult WT or ∆201Ex2 CPC clones. Scale bar: 50 µm. Data represent means ± SEM; *$p < 0.05$ as compared to fetal CPCs in expansion; §$p < 0.05$ compared to the indicated conditions (n=3-6). ANOVA with post-hoc Tukey. See also Supplemental Fig. S1, S2 and S3.

Figure 2. The *CARMEN-201* Exon 2 contains a functional transposable element implicated in SMC specification.

(a) Expression of *CARMEN* isoforms and (b) SMC markers (*MYH11*; *CNN1*; *TAGLN; CALD1*) in differentiating fetal cells either untransfected (None), transfected with the SAM system in the absence of gRNA (SAM) or with the SAM system with a gRNA targeting sequences upstream the *CARMEN* TSS (SAM/gRNA). (c) Representative images and quantification of SMCs in cultures of differentiating fetal CPCs transfected as in (a). Scale bar: 50 µm. (d) Position of the MIRc transposable element in the *CARMEN-201* second exon, and sequence conservation. (e) Expression of *CARMEN-201* using either a primer pair specific for the endogenous transcript (P1) or the exogenous exon 2 (P3), and (f) SMC markers (*MYH11*; *CNN1*; *TAGLN; CALD1*) in differentiating fetal CPCs either not transduced (None), transduced with a lentiviral vector encoding *CARMEN(C)-201* Ex2 or transduced with a lentiviral vector encoding a mutated *C-201* Ex2 (*C-201* mutEx2). (g) Representative images and quantification of SMMHC-positive CNN1-positive SMCs in cultures of differentiating fetal CPCs transfected as in (f). Scale

bar: 50 µm. Data represent means ± SEM; *p < 0.05 as compared to fetal CPCs in expansion; §p < 0.05 compared to the indicated conditions (n=3-6). ANOVA with post-hoc Tukey. See also Supplemental Fig. S3 and S4.

Figure 3. Transcriptomic analysis and identification of upstream regulators of CM and SMC specification in fetal CPCs with or without C-201 Exon 2 overexpression.

(a) Principal Component Analysis (PCA) visualizing transcriptomic data in a two-dimensional space. (b) Expression heatmap of regulators and markers of the CM and the SMC fate. The heatmaps show scaled TPM values. (c-d) TRIAGE transformation of input RNA-Seq data predicts regulatory genes controlling cell differentiation based on TRIAGE rank order (left) compared to ranking observed using simple gene expression (right). Control differentiation (None) vs. differentiation following C-201 Exon 2 overexpression (C-201 Ex2) 1 (d1) or 7 days (d7) after transduction. Regulators implicated in cardiovascular differentiation are highlighted in red. (e) Human heart single-cell data analysis reveals genes positively and negatively correlated with *CARMEN* expression during development. (f) UMAP plots showing epicardium-, pericyte- and SMC-specific expression of *CARMEN* in the human heart 6.5 weeks post-conception. See also Supplemental Fig. S4 and S5.

Figure 4. Identification of *CARMEN-201* protein partners.

(a) Quantification of REST, (b) NSUN6 and (c) RPA1 by Western blotting in a protein pulldown assay using biotinylated sense or antisense *CARMEN-201* transcript in adult CPC lysates. Graphs show means ± SEM *p < 0.05 as compared to input; §p < 0.05 comparing sense and antisense probe (n = 3). (d-f) Quantification of *CARMEN-201* enrichment after RNA immunoprecipitation using a control immunoglobulin G (IgG) or IgG directed against REST (anti-REST IgG), NSUN6 (anti-NSUN6 IgG) and RPA1 (anti-RPA1 IgG). Graphs show means ± SEM; *p < 0.05 as compared to control (n=3). (g) Expression of *REST*, *CARMEN-201* and SMC markers (*MYH11*; *CNN1*; *TAGLN*) in differentiating fetal CPCs either not transduced (None), transduced with a lentiviral vector encoding *C-201* Exon 2 (*C-201* Ex2), and treated with either a scrambled siRNA (Scr siRNA) or a siRNA directed against REST (Anti-*REST* siRNA). (h) Representative images and quantification of SMMHC-positive CNN1-positive SMCs

and ACTN2-psoitive CMs in cultures of differentiating fetal CPCs transfected as in (g). Scale bars: 50 µm. Data represent means ± SEM; *p < 0.05 as compared to fetal CPCs in expansion; §p < 0.05 compared to indicated conditions (n=3-6). ANOVA with post-hoc Tukey. See also Supplemental Fig. S6.

Figure 5. Identification of *IRX1*, *IRX5*, *SFRP1* and *ISL1* as target genes of *C-201* action

(a) Significant DNA-binding domains (DBD) identified in the mature sequence of C-201 and C-205 when analyzed against the differentially downregulated genes on day 1 and day 7 following induction of differentiation. Graph shows the number of DNA-binding sites (DBS) for each DBD. (b) Venn diagram illustrating the overlap of promoters predicted to form triple helices with *C-201* and *C-205*. Functional enrichment analysis of the isoform-specific bound promoters. Graph shows the negative logarithm of the P value. (c) Venn diagram illustrating the identification of *IRX1*, *IRX5*, *ISL1* and *SFRP1* as common to the indicated lists of genes. Hypergeometric tests were performed to explore the significance of the overlap (d) REST occupancy at the promoters of *IRX1*, *IRX5*, *SFRP1* and *ISL1* in adult CPCs with or without GapmeR-mediated *C-201* silencing as determined by ChIP-qPCR. Occupancy at the *GAPDH* and the *SYN1* promoters was used as negative and positive controls respectively. (e) Expression of *IRX1, IRX5, ISL1* and *SFRP1* in differentiating fetal cells either untransfected (None), transfected with the SAM system in the absence of gRNA (SAM) or with the SAM system with a gRNA targeting sequences upstream the *CARMEN* TSS (SAM/gRNA). (f) Expression of *IRX1, IRX5, ISL1* and *SFRP1* in differentiating adult CPCs treated with Scrambled siRNA (Scr SiRNA) or Anti-*REST* siRNA. (g) Expression of *IRX1, IRX5, ISL1* and *SFRP1* in differentiating fetal CPCs either untransfected, transfected with a lentiviral vector encoding *C-201* Ex2 or a mutated *C-201* Ex2 (*C-201* mutEx2), treated with either a scrambled siRNA (Scr siRNA) or a siRNA directed against REST (Anti-*REST* siRNA). Data represent means ± SEM; *p < 0.05 as compared to CPCs in expansion; §p < 0.05 compared to indicated conditions (n=3-6). ANOVA with post-hoc Tukey. See also Supplemental Fig. S7.

Figure 6. Validation of candidate cardiogenic factor downregulation

(a-d) Expression of epicardial genes (*WT1, TCF21, TBX18*) in differentiating fetal CPCs following *IRX1*, *IRX5*, *ISL1* and *SFRP1* silencing. (e) Epicardial (*WT1, TCF21, TBX18*) SMC (*MYH11, TAGLN, CNN1*)

and CM marker (*MYH6*) expression in differentiating fetal CPCs overexpressing *C-201* Ex2, and in fetal CPCs treated with siRNAs directed against the indicated factors in combination. (f) Representative images and quantification of ACTN2-positive CMs and SMMHC-positive CNN1-positive SMCs in cultures of differentiating fetal CPCs transfected as in (e). Scale bars: 50 µm. Expression of *CARMEN-201 (C-201)*, *CARMEN-205 (C-205)* and *CARMEN-217 (C-217)* in differentiating fetal CPCs treated as in (e). Data represent means ± SEM; *p < 0.05 as compared to fetal CPCs in expansion; §p < 0.05 as compared to fetal CPCs in differentiation (n=6-12). ANOVA with post-hoc Tukey. See also Supplemental Fig. S8.

Figure 7. *CARMEN-201* expression is increased in response to myocardial infarction in humans

(a) Association of *CARMEN* with cardiovascular traits using CTG-VIEW. (b-e) Detection of *C-201* in the failing human heart by RNA in situ hybridization assay (BaseScope). (b and c) Representative images of sections of an explanted heart obtained from a heart failure patient. (b). Top: Hematoxylin/Eosin; scale bar: 500 µm; Bottom: Masson Trichrome staining; scale bar: 500 µm. (c) Left: Masson Trichrome staining; scale bar: 100 µm; Right: Hematoxylin/Eosin; scale bar: 20 µm. Red dots: Positive *C-201* BaseScope signals. (d-e) Quantification of *C-201* expression in CMs and mural cells. Data represent means ± SEM; *p < 0.05; ANOVA with post-hoc Tukey. Two patients; 5 sections per patient; 5 to 10 different areas per section. LV: Left ventricle; RV: Right ventricle; LA: Left atria; RA: Right atria. (f) Immunostaining detection of VIMENTIN-positive cells (endothelial cells and fibroblasts) and SMMHC-positive cells (SMCs) in adjacent sections of that used in b and c; scale bar: 25 µm. (g) Time course of blood sample collection, and expression of *C-201* in plasma of STEMI and NSTEMI patients (Data represent means ± SEM; n=11; *p< 0.01; ANOVA with post-hoc Tukey), and Table presenting patient characteristics. See also Supplemental Fig. S8.

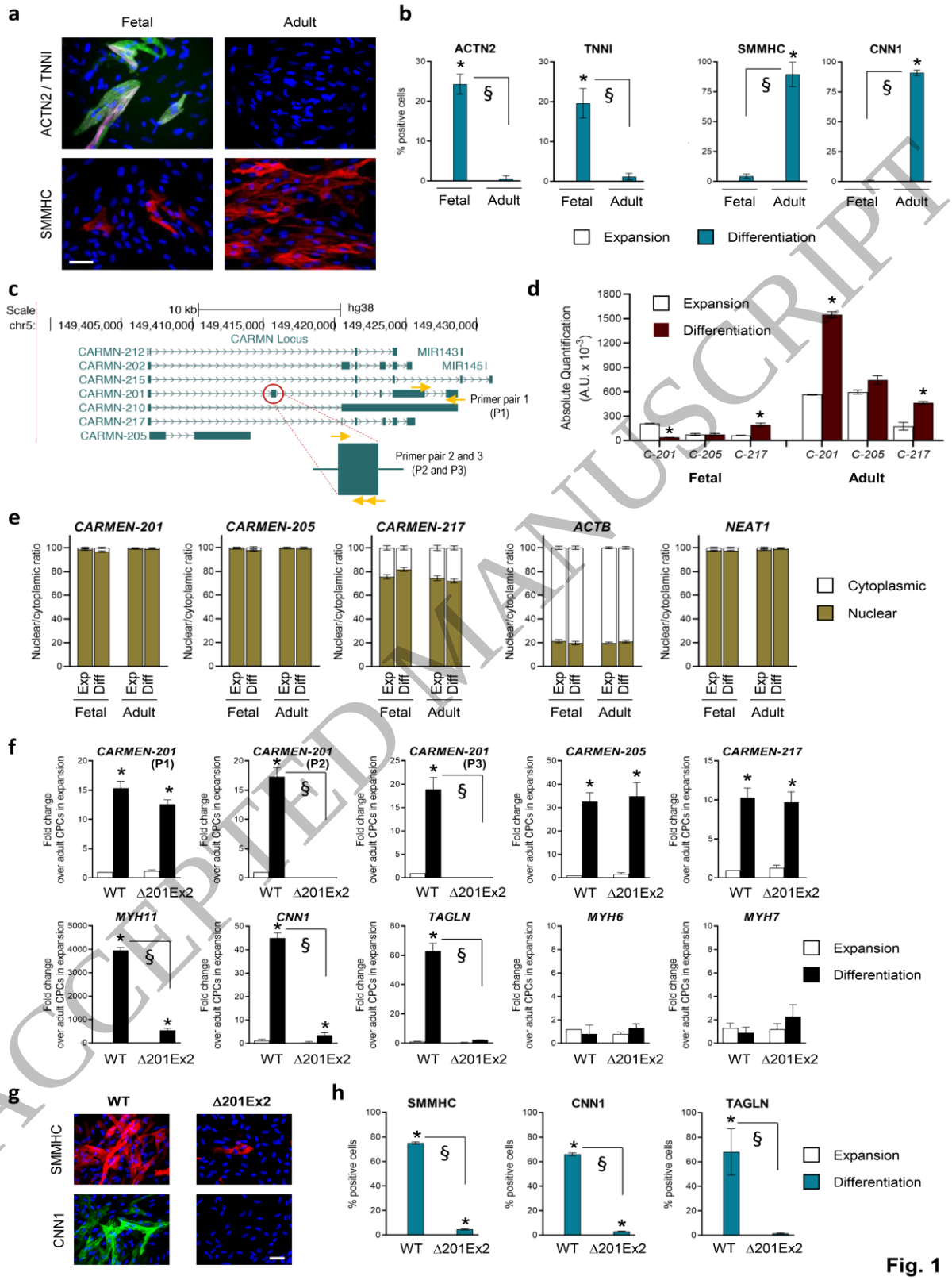

Fig. 1

Figure 1
160x231 mm (x DPI)

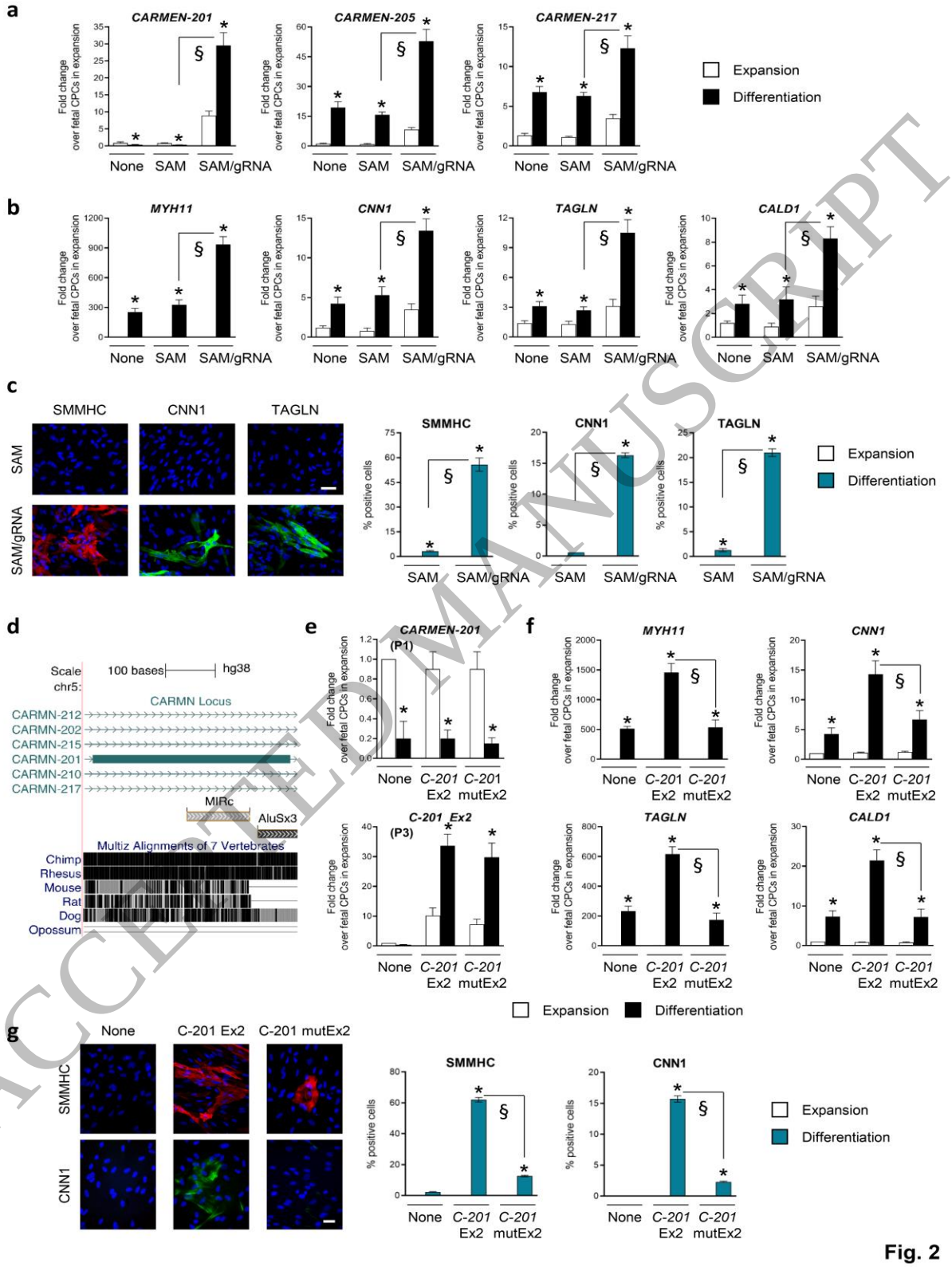

Fig. 2

Figure 2
160x231 mm (x DPI)

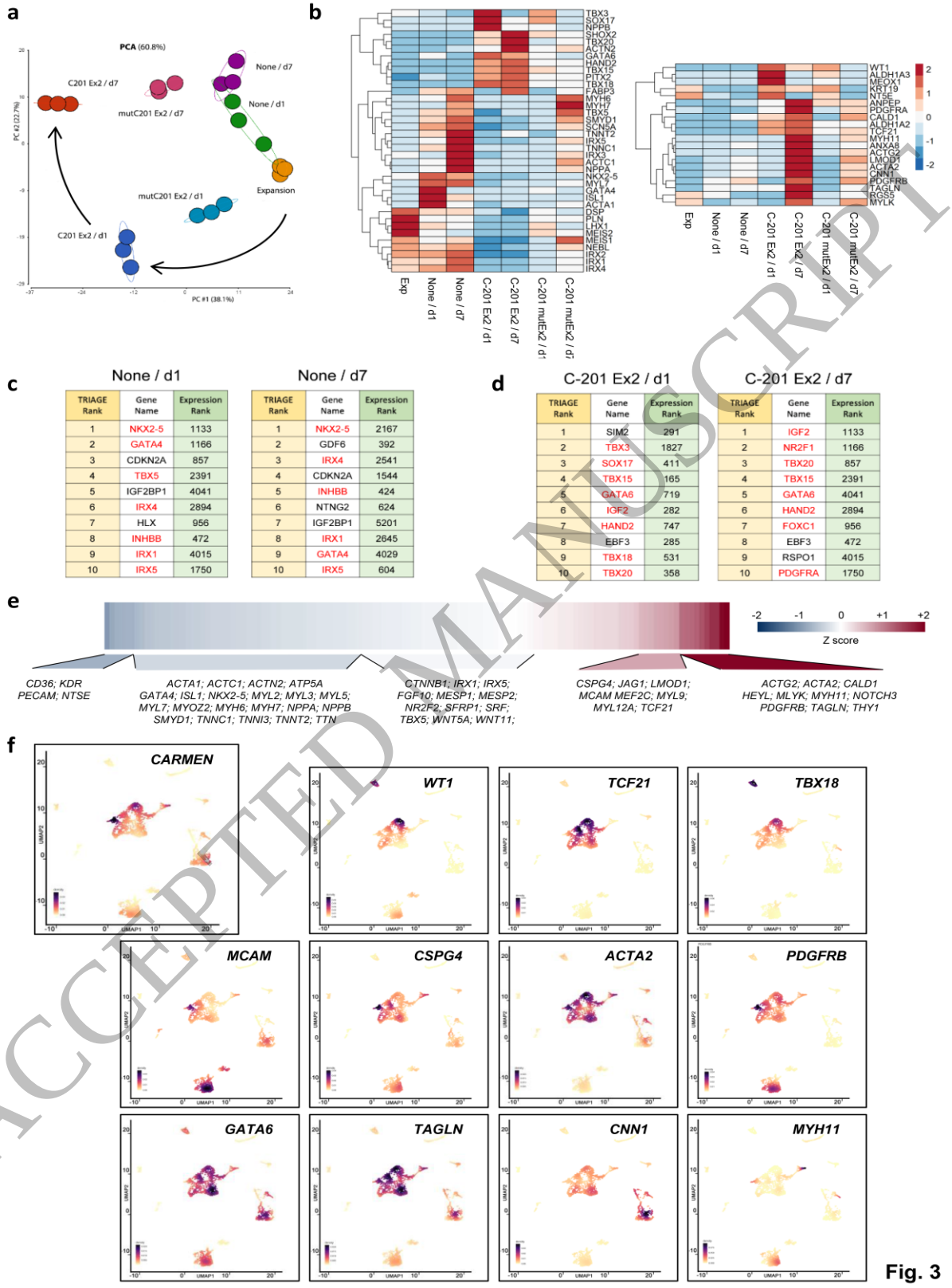

TRIAGE Rank	Gene Name	Expression Rank
1	NKX2-5	1133
2	GATA4	1166
3	CDKN2A	857
4	TBX5	2391
5	IGF2BP1	4041
6	IRX4	2894
7	HLX	956
8	INHBB	472
9	IRX1	4015
10	IRX5	1750

TRIAGE Rank	Gene Name	Expression Rank
1	NKX2-5	2167
2	GDF6	392
3	IRX4	2541
4	CDKN2A	1544
5	INHBB	424
6	NTNG2	624
7	IGF2BP1	5201
8	IRX1	2645
9	GATA4	4029
10	IRX5	604

TRIAGE Rank	Gene Name	Expression Rank
1	SIM2	291
2	TBX3	1827
3	SOX17	411
4	TBX15	165
5	GATA6	719
6	IGF2	282
7	HAND2	747
8	EBF3	285
9	TBX18	531
10	TBX20	358

TRIAGE Rank	Gene Name	Expression Rank
1	IGF2	1133
2	NR2F1	1166
3	TBX20	857
4	TBX15	2391
5	GATA6	4041
6	HAND2	2894
7	FOXC1	956
8	EBF3	472
9	RSPO1	4015
10	PDGFRA	1750

Fig. 3

Figure 3
160x231 mm (x DPI)

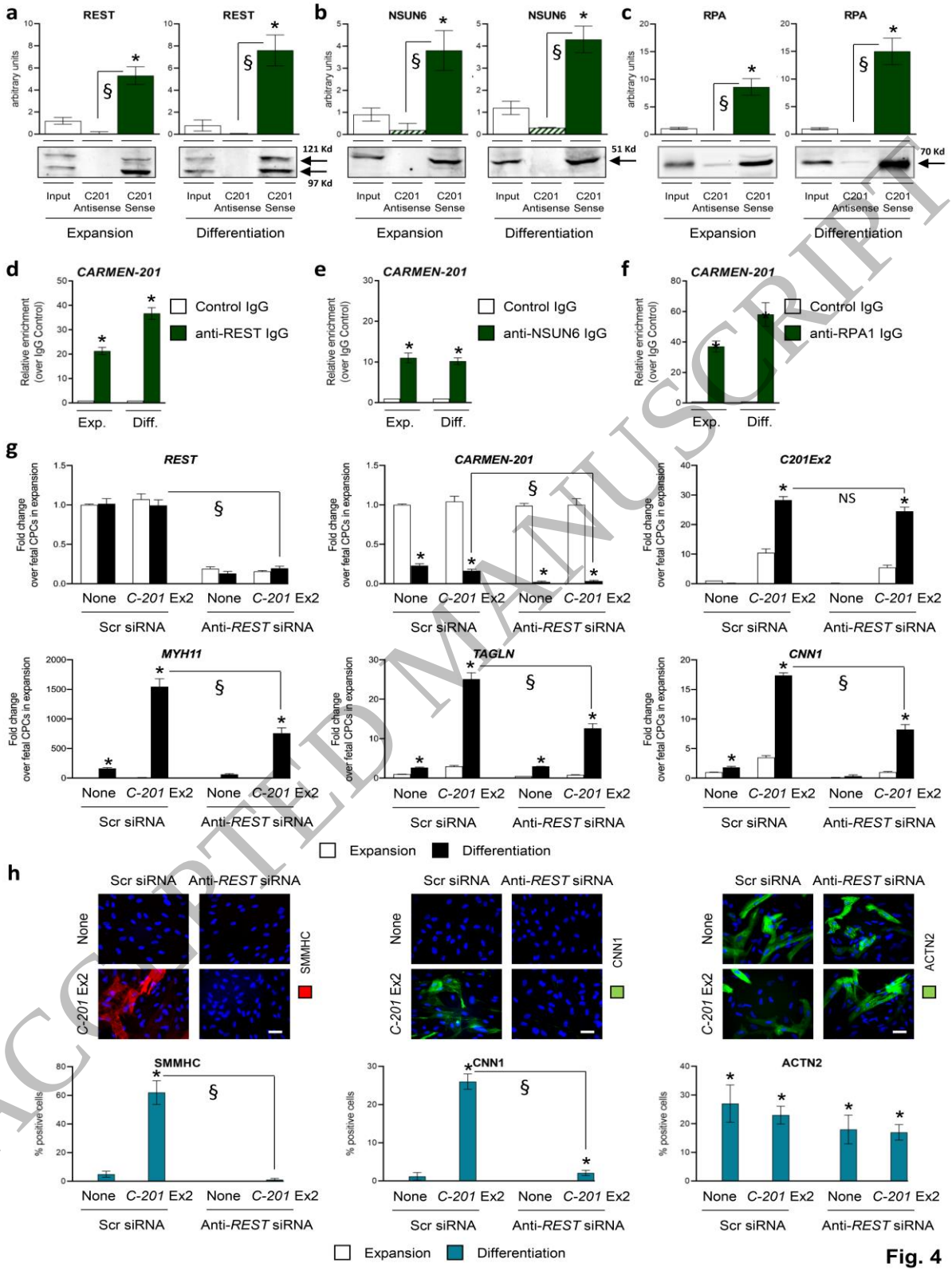

Fig. 4

Figure 4
160x231 mm (x DPI)

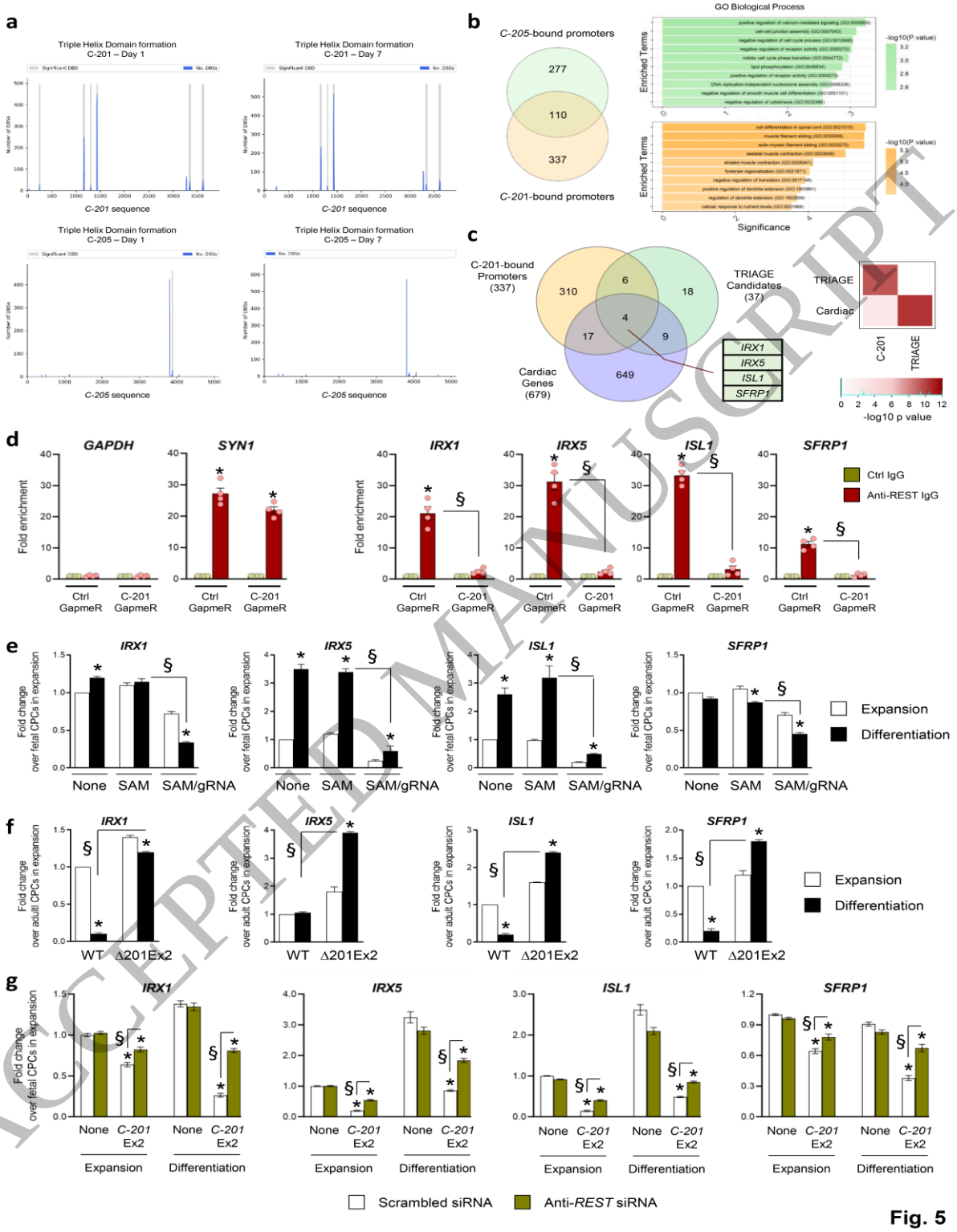

Fig. 5

Figure 5
160x231 mm (x DPI)

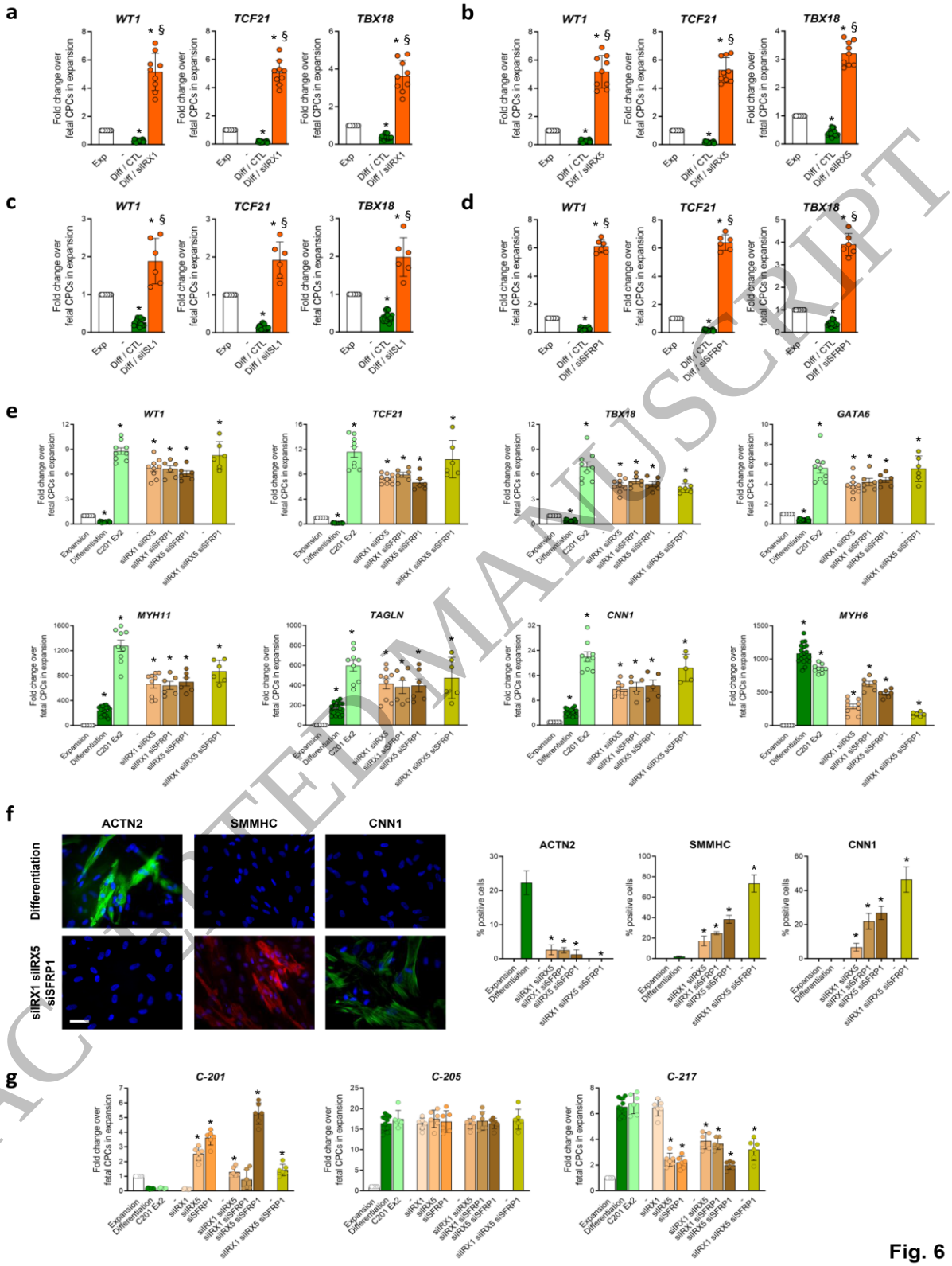

Fig. 6

Figure 6
160x231 mm (x DPI)

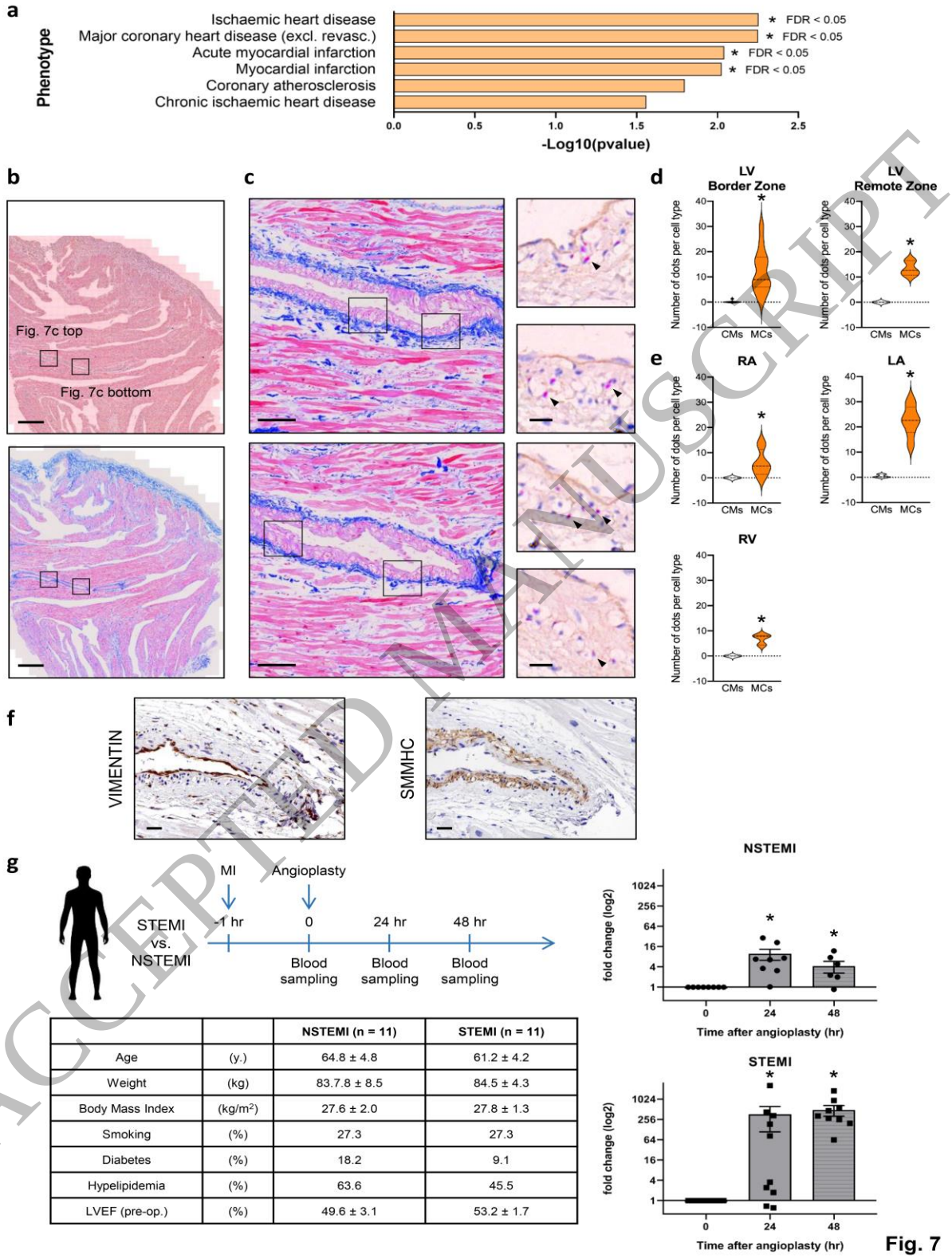

		NSTEMI (n = 11)	STEMI (n = 11)
Age	(y.)	64.8 ± 4.8	61.2 ± 4.2
Weight	(kg)	83.7.8 ± 8.5	84.5 ± 4.3
Body Mass Index	(kg/m^2)	27.6 ± 2.0	27.8 ± 1.3
Smoking	(%)	27.3	27.3
Diabetes	(%)	18.2	9.1
Hypelipidemia	(%)	63.6	45.5
LVEF (pre-op.)	(%)	49.6 ± 3.1	53.2 ± 1.7

Fig. 7

Figure 7
160x231 mm (x DPI)

1

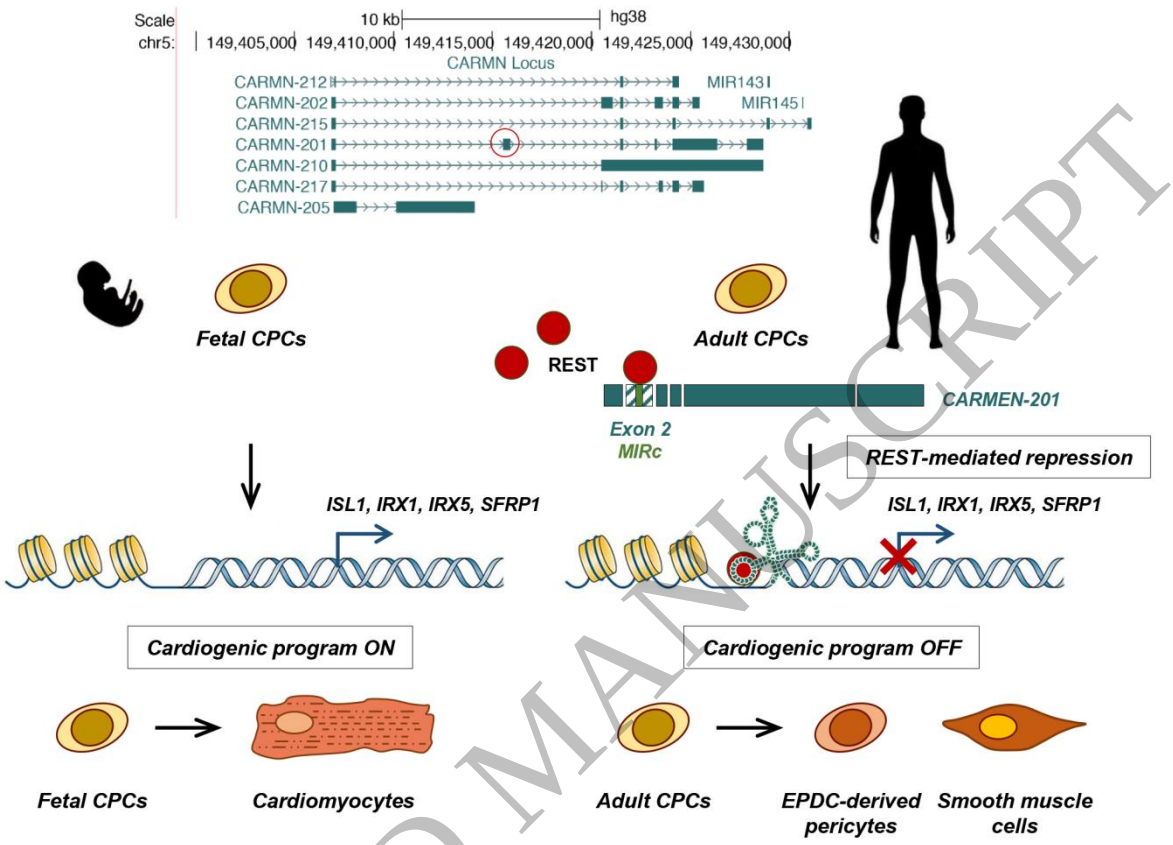

2

3 **Graphical Abstract**